Supporting Information for

Antenna Effect in BODIPY-(Zn)Porphyrin entities Promotes H_2 Evolution in Dye-sensitized Photocatalytic Systems

Vasilis Nikolaou,[a] Georgios Charalambidis,[a] Georgios Landrou[a], Emmanouil Nikoloudakis,[a] Aurélien Planchat,[b] Ronilnta Tsalameni,[a] Karen Junghans,[c] Axel Kahnt,[c]* Fabrice Odobel,[b]* and Athanassios G. Coutsolelos[a]**

[a] Laboratory of Bioinorganic Chemistry, Department of Chemistry, University of Crete, Voutes Campus, 70013 Heraklion, Crete, Greece.

[b] Université de Nantes, CNRS, Chimie et Interdisciplinarité: Synthèse, Analyse, Modélisation (CEISAM), UMR 6230, 2 rue de la Houssinière, 44322 Nantes cedex 3, France.

[c] Leibniz Institute of Surface Engineering (IOM), Permoserstr, 15, 04318 Leipzig, Germany.

* Corresponding authors: acoutsol@uoc.gr

fabrice.Odobel@univ-nantes.fr

axel.kahnt@iom-leipzig.de

v.nikolaou@uoc.gr

Table of contents

Experimental Section.

General information. All the reagents and the solvents were purchased from usual commercial sources and used without further purification, unless otherwise stated. The ^{1}H NMR spectra of the compounds were recorded on Bruker AMX-500 MHz and Bruker DPX-300 MHz spectrometers, respectively. The solution of the sample was in deuterated solvent by using the solvent peak as the internal standard. High-resolution mass spectra were recorded on a Bruker ultrafleXtreme MALDI-TOF spectrometer, using trans-2-[3-(4-tert-butylphenyl)-2-methyl-2-propenylidene] malononitrile as matrix. The 0.5 wt% platinized TiO_2 nanoparticles (platinum doped TiO_2 nanoparticles, Pt-TiO_2) were prepared according to already published experimental procedures.[1]

Photophysical Measurements. The UV-Vis absorption spectra of all porphyrinoids in solution were obtained using a Shimadzu UV-1700 spectrophotometer in quartz cuvettes of 1 cm path-length. The absorption spectra in their solid state upon the adsorption onto the TiO_2 nanoparticles were obtained onto quartz slides 2x2 cm^2 using a UV/Vis/NIR Lambda 19, Perkin-Elmer spectrophotometer. The emission spectra were measured on a JASCO FP-6500 fluorescence spectrophotometer equipped with a red-sensitive WRE-343 photomultiplier tube (wavelength range: 200-850 nm). Nanosecond resolved transient absorption measurements were performed using the output of the forth harmonic (266 nm) of a Nd:YAG laser (Quanta-Ray GCR-11 - Spectra Physics). Pulse widths of 5 ns and energies between 4 and 5 mJ per pulse were selected. The transient absorption detection is based on a pulsed (Pulse MSP05 - Müller-Elektronik-Optik) Xenon lamp (XBO 150,Osram), a monochromator (Spectra Pro 275, Acton Research), R9220 photomultiplier tube (Hamamatsu

Photonics) and a 1 GHz digital oscilloscope (TDS 684 A, Tektronix). The laser power of every laser pulse was registered using a fast Silicon photodiode.

Light on/light off photo-current experiments.

Preparation of dye-sensitized TiO_2 films: FTO conductive glass substrates (F-doped SnO_2) were cleaned by successive sonication in soapy water, then in an ethanolic solution of HCl (0.1 M) for 10 minutes, and finally dried in air. TiO_2 films were prepared in three steps. A first treatment is applied by immersion for 30 min in an aqueous $TiCl_4$ solution at 80°C. Three successive layers of mesoporous TiO_2 were then screen printed using a transparent colloidal paste (Dyesol DSL 18NR-T) and a final light scattering layer (Dyesol DSL 18NR-AO) was affixed, with 20-minute long drying steps at 150 °C between each layer. The obtained substrates were then sintered at 450 °C, following a progressive heating ramp (325 °C for 5 min, 375 °C for 5 min, 450 °C for 30 min). A second $TiCl_4$ treatment was immediately conducted afterwards and the electrodes were fired one last time at 450 °C for 30 minutes. Thicknesses (16 µm) were measured by a Sloan Dektak 3 profilometer. For the absorption spectra, only one layer of transparent colloidal paste (Dyesol DSL 18NR-T) was deposited on glass. The prepared TiO_2 electrodes were soaked while still hot (ca. 80 °C) in a 0.2 mM solution of the dye in THF/MeOH : 1/1 mixture for 3 hours. The electrodes were rinsed with THF/MeOH: 1/1 mixture and dried with a jet of nitrogen. For axial ligation of **BDP(Im)**, the TiO_2 electrodes coated with the porphyrin derivative was soaked in a 0.2 mM solution of **BDD(Im)** in acetonitrile for 30 minutes and then, it was rinsed with acetonitrile before being dried by a jet of nitrogen.

Chopped light photocurrent measurements were performed with an integrated photoelectrochemical workstation from Zahner (ZAHNER- Elektrik GmbH & Co.

KG, Germany), containing a first potentiostat for the light control and a second potentiostat (Zenium) for the electrochemical control all run under Thales software. A standard three electrode configuration with $Hg/HgSO_4$, coiled Pt-wire and a film of TiO_2 sensitized with the dye (area 0.25 cm^2) were used as the reference, counter and working electrodes, respectively. A white light lamp (1088wlr02, ZAHNER- Elektrik GmbH & Co. KG, Germany, spectrum given in **Figure S12**) was used as the light source (350W/m) and was periodically switched on and off (duration 5 s), while the potential was swept at a rate of 5 mV/s.

Determination of Incident Photon to Current Efficiency (IPCE).

IPCE spectra were measured with Zahner system (Zahner CIMPS) equipped with the tunable light source TLS03. A standard three electrode configuration with $Hg/HgSO_4$, coiled Pt-wire and a film of PMI coated TiO_2 film (area 0.25 cm^2) were used as the reference, counter and working electrodes, respectively. During IPCE measurements, the TiO_2 film was biased at 0 V *vs.* SCE reference electrode using wideband illumination LEDs, a background light and light was chopped at a frequency of 1 Hz.

Adsorption of chromophores onto Pt-TiO_2.

Our first objective was to determine the adsorption percentage of all chromophores anchored onto the Pt-TiO_2 nanoparticles. Therefore, we thoroughly investigated the adsorption of **BDP**, **Por**, **BDP-Por** dyad and **Por/BDP** (1:1 mixture) onto the Pt-TiO_2 surface using absorption spectroscopy. For this study, we prepared 2 mL solutions of standard concentration in THF (see table S1) and recorded their absorption features. As illustrated in **Figure S7**, in each solution 10 mg of Pt-TiO_2 were added and the solution was sonicated for 5 minutes, stirred for 60 minutes and lastly centrifuged for

4 minutes in 13000 revolutions per minute (rpm). The amount of the absorbed porphyrin onto the TiO_2 nanoparticles was quantified by studying the absorbance of each supernatant solution before and after the adsorption.

Photocatalytic measurements.

The photocatalytic H_2 evolution studies were performed in a glass vial (10 mL) sealed with a rubber septum, at ambient temperature and pressure. Before each experiment, a fresh buffer solution was prepared. In detail, the buffer solution was a 1M aqueous solution of ascorbic acid (AA) that was adjusted to pH=4 using aqueous solution of NaOH. In the glass vial, 5 mL of the buffer solution together with 10 mg of dye-Pt-TiO_2 were added. In order to ensure anaerobic conditions, the suspensions were degassed using nitrogen for 5 min (in an ice/water bath). Finally, the vials were sealed with a silicon septum and were irradiated under continuous stirring. For the photo-excitation of the samples, a low power white LED lamp ring of 40 W, with color temperature of 6400 K and lumen of 3800 LM was used.

The H_2 evolution was determined using gas chromatography (GC) using a Shimadzu GC 2010 plus chromatograph with a TCD detector and a molecular sieve 5 Å column (30 m - 0.53 mm). For every measurement, 100 μL were taken from the headspace of the vial and were instantly injected in the GC. In all cases, both the reported H_2 production values and the Turn Over Number (TON) are the average of three independent experiments.

Calculation of TONs and H_2 evolution mmol(H_2) g(cat)$^{-1}$ h^{-1}

The TONs were calculated according to the following equation:

$$\mathbf{TON} = \frac{n(\mathrm{H_2})}{n(\mathrm{PS})}$$

Where: ***n*(H$_2$)** is the total amount of the produced H_2 (in mmol) and ***n*(PS)** is the total amount of the photosensitizer (in mmol).

In every photocatalytic experiment 0.01 g of Pt-TiO_2 (0.5% (w/w) of Pt) were used. Thus, the final amount of the catalyst (Pt) in each experiment is 0.00005 g. The H_2 evolution rate was calculated according to the equation:

$$\textbf{H}_2\ \textbf{evolution mmol(H}_2\textbf{) g(cat)}^{-1}\ \textbf{h}^{-1} = \frac{n(\mathrm{H_2})}{m(\mathrm{Catalyst})\ \mathrm{x}\ t}$$

Where: **n(H$_2$)** is the total amount of the produced H_2 (in mmol), **m(catalyst)** is the total amount of Pt (in grams) and **t** is the irradiation time in hours (t = 24 h).

Synthesis and Characterization.

Synthesis of Zn-TMP(COOMe): To a CH_2Cl_2 solution (20 mL) of TMP(COOMe)[2] (50 mg, 0.063 mmol), a MeOH (3 mL) solution containing $Zn(CH_3COO)_2 \cdot 2H_2O$ (219 mg, 1 mmol) was added and the reaction mixture was stirred at room temperature overnight. The volatiles were evaporated, the porphyrin was diluted in $CHCl_3$ (25 mL) and washed with H_2O (3 x 25 mL). The solvent was consequently removed under reduced pressure and the produced porphyrin then purified by column chromatography (silica gel, CH_2Cl_2/Hexane 6:4) yielding 51 mg of Zn-TMP(COOMe) (0.059 mmol, yield: 94%).

^{1}H NMR (500 MHz, $CDCl_3$): δ = 8.80 (d, *J* = 4.6 Hz, 2H), 8.77 (d, *J* = 4.6 Hz, 2H), 8.72 (s, 4H), 8.40 (d, *J* = 8.1 Hz, 2H), 8.31 (d, *J* = 8.1 Hz, 2H), 7.28 (s, 6H), 4.09 (s, 3H), 2.63 (s, 9H), 1.86 (m, 18H) ppm.

HRMS-(MALDI-TOF): m/z calc. for $[M]^+$ $C_{55}H_{48}N_4O_2Zn$ 860.3069, found 860.3072.

Synthesis of Zn-TMP(COOH), (Por): To a solution of Zn-TMP(COOMe) (40 mg, 0.046 mmol) in 22 mL of a THF/MeOH mixture (2:1), an aqueous solution (7 mL) of

KOH (100 mg, 1.78 mmol) was added. The reaction mixture was stirred at room temperature overnight. The solvents were evaporated under reduced pressure and distilled H_2O (5 mL) was added to the resulting residue. Acidification of the mixture by using HCl (aq) 1 M resulted in the precipitation of a solid which was filtered, washed with distilled H_2O and dried yielding 35 mg of **Por** (0.041 mmol, 90%).

^{1}H NMR (500 MHz, $CDCl_3$): δ = 8.81 (d, *J* = 4.5 Hz, 2H), 8.78 (d, *J* = 4.6 Hz, 2H), 8.71 (s, 4H), 8.49 (d, *J* = 7.8 Hz, 2H), 8.35 (d, *J* = 7.9 Hz, 2H), 7.28 (s, 6H), 2.63 (m, 9H), 1.85 (m, 18H) ppm.

HRMS-(MALDI-TOF): m/z calc. for $[M]^+$ $C_{54}H_{46}N_4O_2Zn$ 846.2912, found 846.2918.

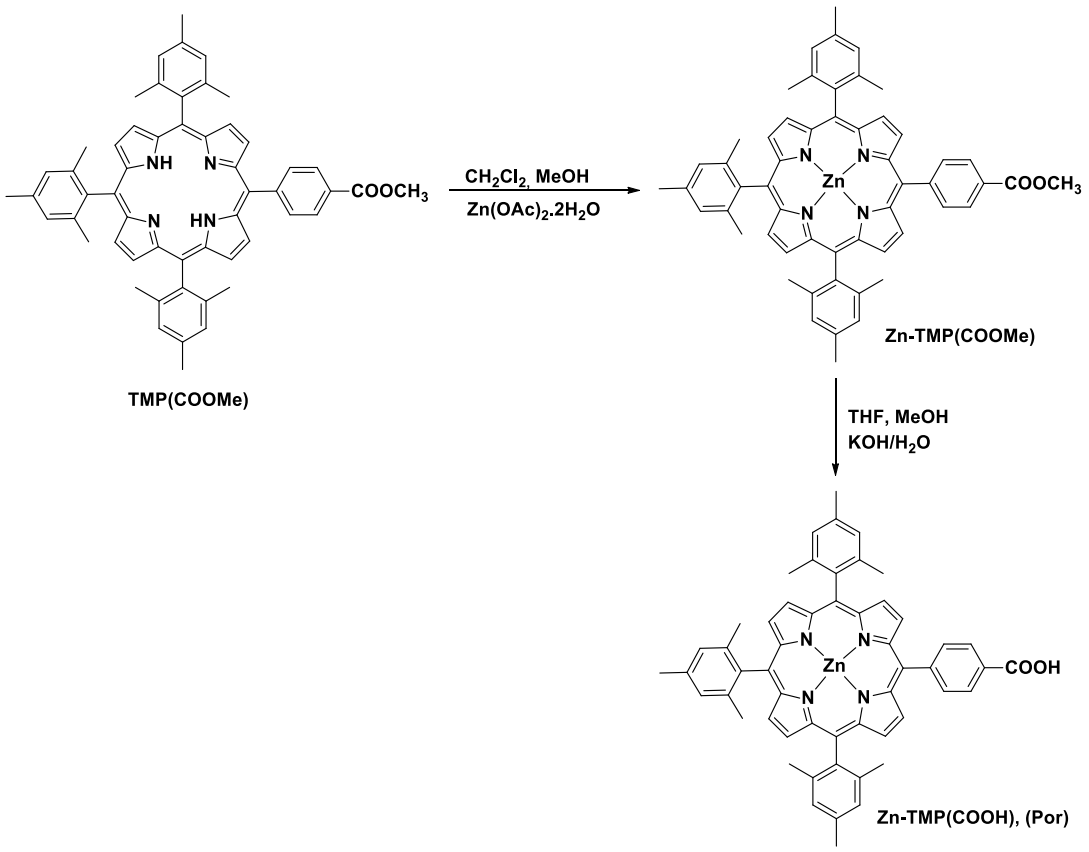

Scheme S1. The synthetic approach followed for the preparation of **Por**.

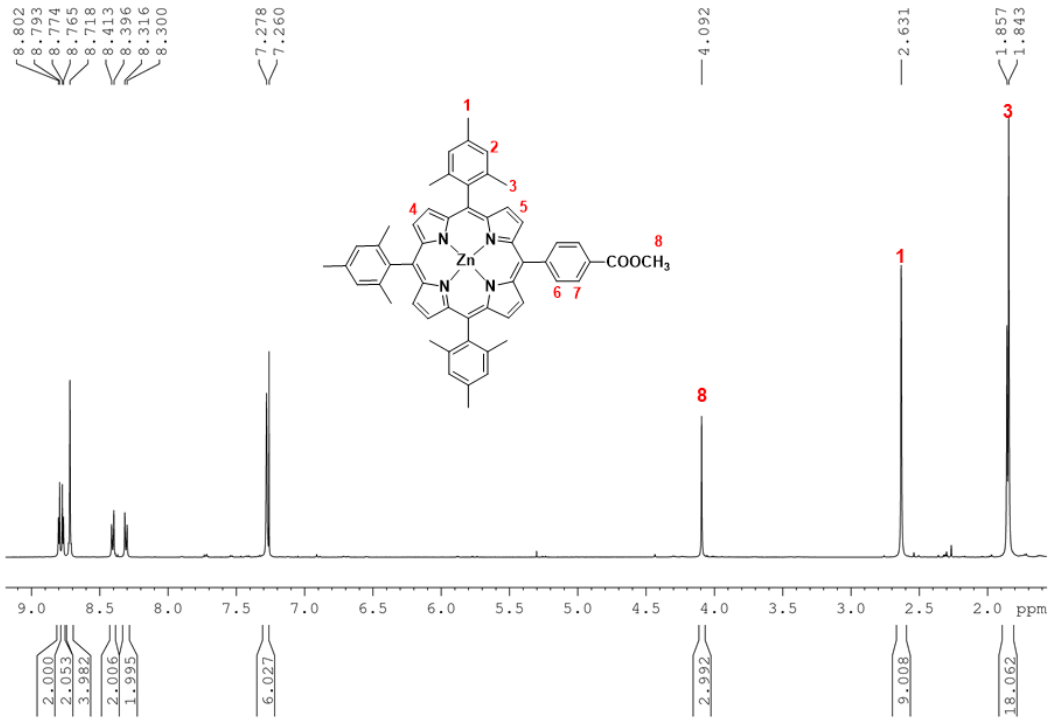

Figure S1. ^{1}H NMR spectrum of **TMP(COOMe)** (500 MHz, $CDCl_3$).

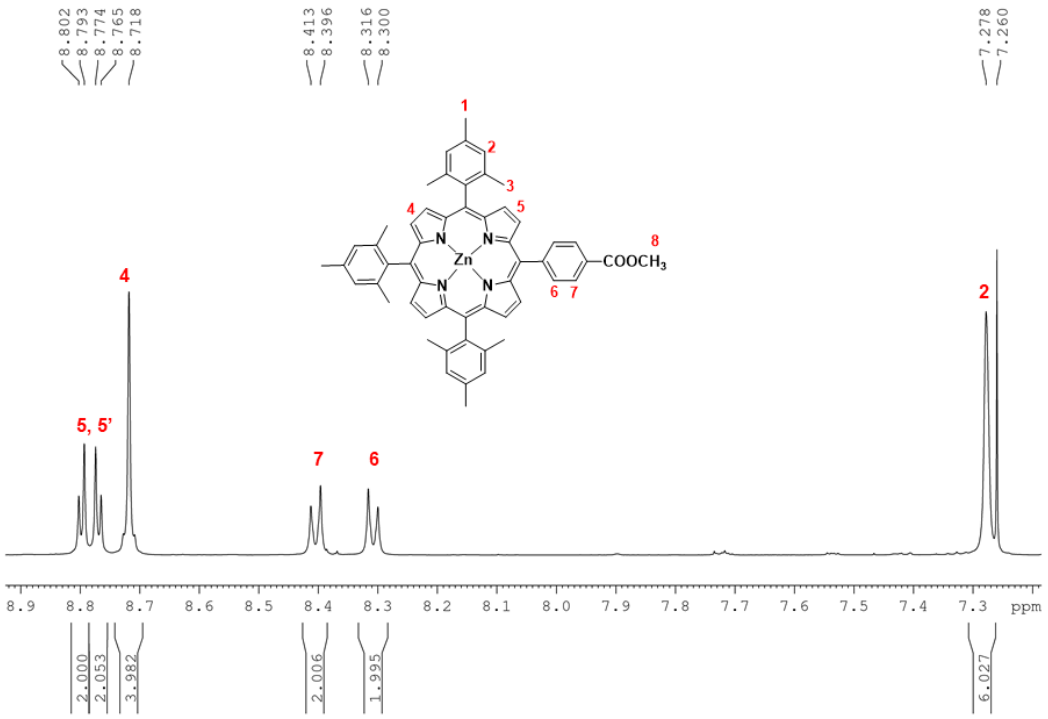

Figure S2. Focus on the aromatic region of the ^{1}H NMR spectrum of **TMP(COOMe)** (500 MHz, $CDCl_3$).

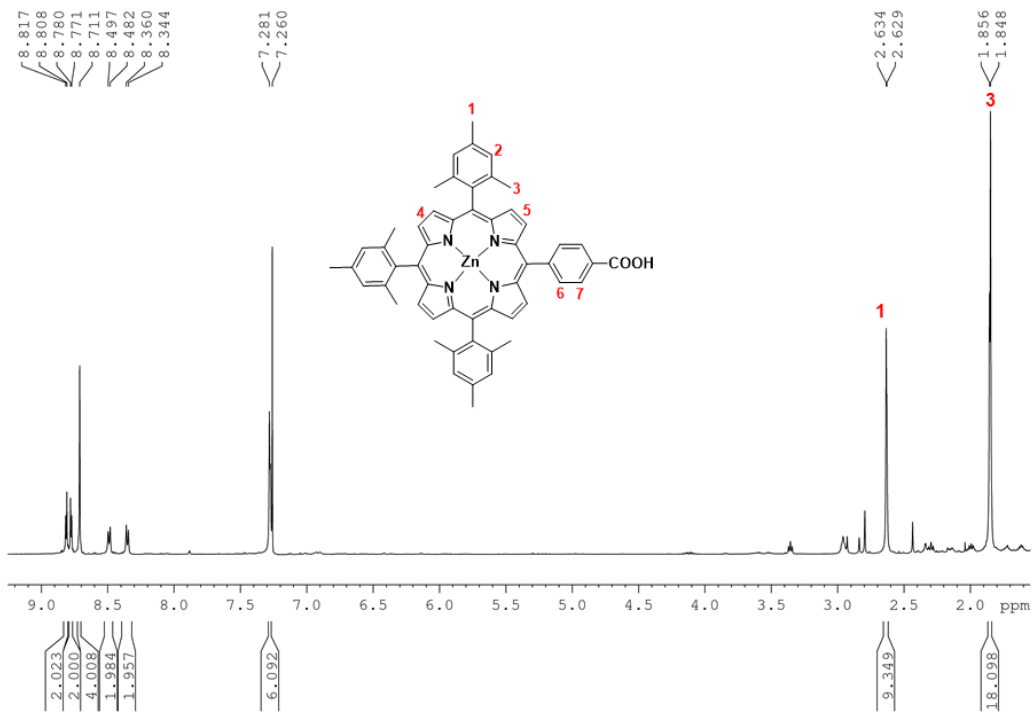

Figure S3. ^{1}H NMR spectrum of Zn-TMP(COOH), (**Por**) (500 MHz, $CDCl_3$).

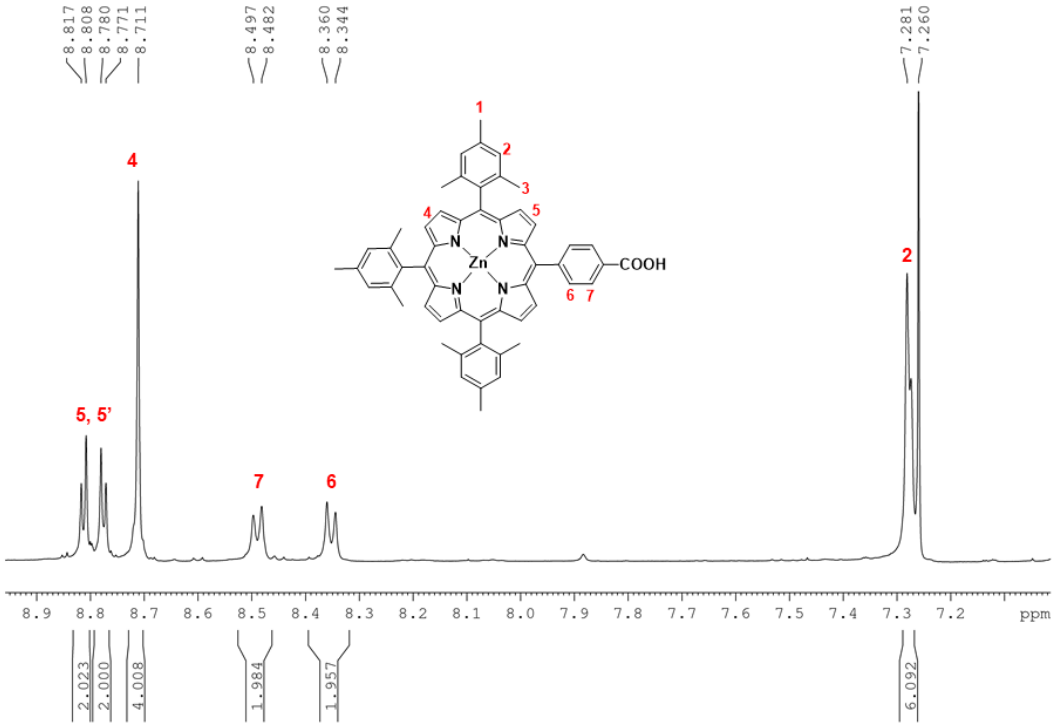

Figure S4. Focus on the aromatic region of the ^{1}H NMR spectrum of Zn-TMP(COOH), (**Por**) (500 MHz, $CDCl_3$).

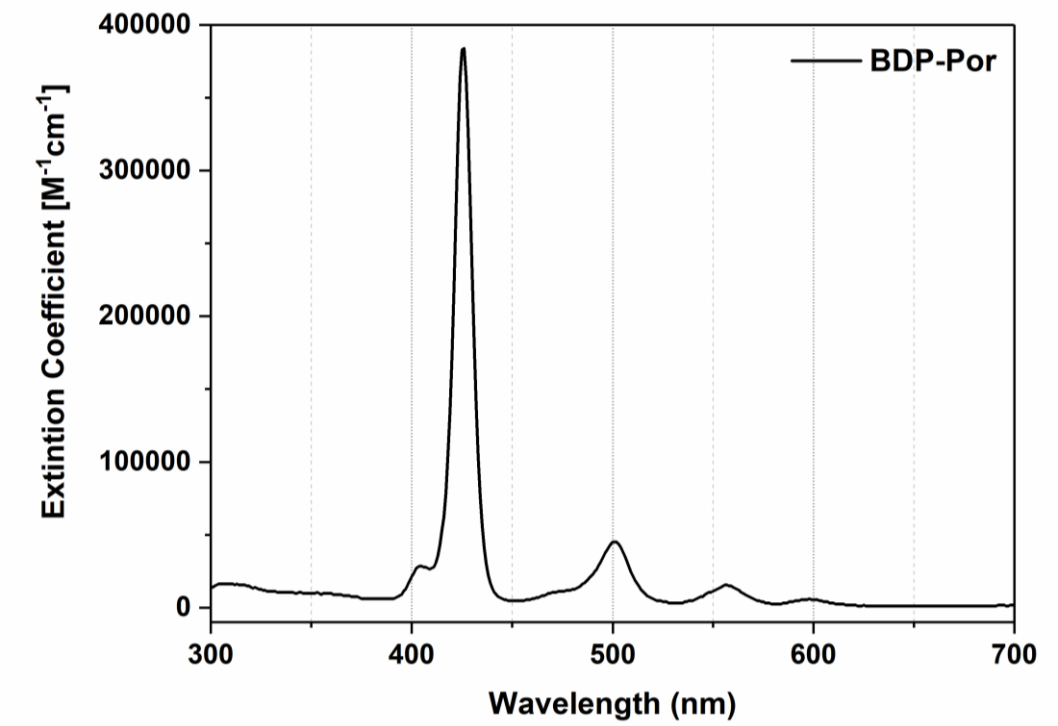

Figure S5. Normalized absorption spectrum of **BDP-Por** dyad in THF.

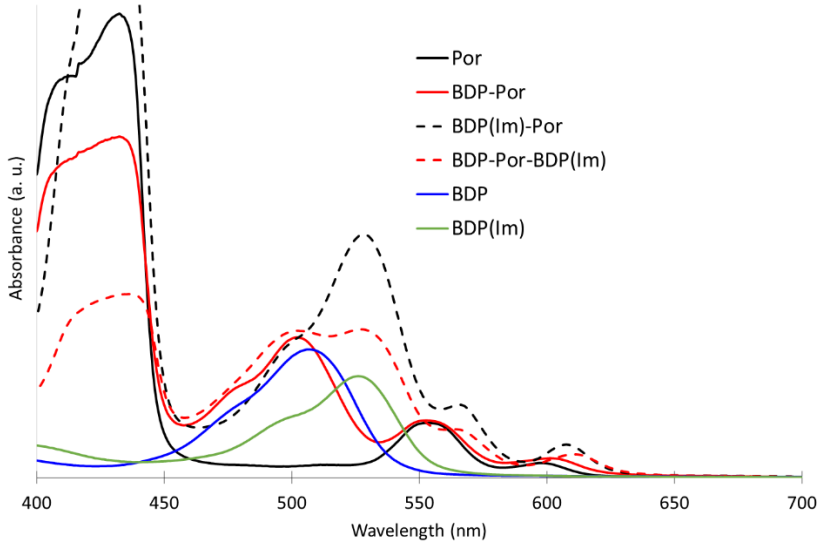

Figure S6. Absorption spectra of the dyes recorded after their chemisorption on thin nanocrystalline TiO_2 films (4 μm).

Table S1. Summary of the photocatalytic H_2 evolution results.

Sample	Concentration (M)[a]	DL (%)[b]	PS (mole)[c]	TON[d]	Activity (mmol g^{-1} h^{-1})[e]
BDP-Por	$2.3x10^{-4}$	91	$4.15x10^{-7}$	640	100
	$1.0x10^{-4}$	91	$1.83x10^{-7}$	900	75
	$4.2x10^{-5}$	95	$8.00x10^{-8}$	1,700	35
	$3.6x10^{-5}$	97	$7.00x10^{-8}$	2,500	70
	$1.2x10^{-5}$	97	$2.30x10^{-8}$	17,500	115
	$5.0x10^{-6}$	99	$1.00x10^{-8}$	15,300	65

[a]The concentration of the initial solutions (2 mL in THF) that were used for the adsorption of the dye (stained solutions), [b]Dye-loading percentage (DL), [c]The amount of the photosensitizer (PS) in each photocatalytic experiment upon its adsorption, [d]The maximum turnover number (TON) of H_2 which was calculated as the number the produced mole of H_2 divided by the number of mole of PS attached onto Pt-TiO_2 (see page S6 for details) and [e]Initial photocatalytic activity defined as the milimole of H_2 evolved per gram of Pt per hour in the first 24 hours (see pages S6-S7 for details).

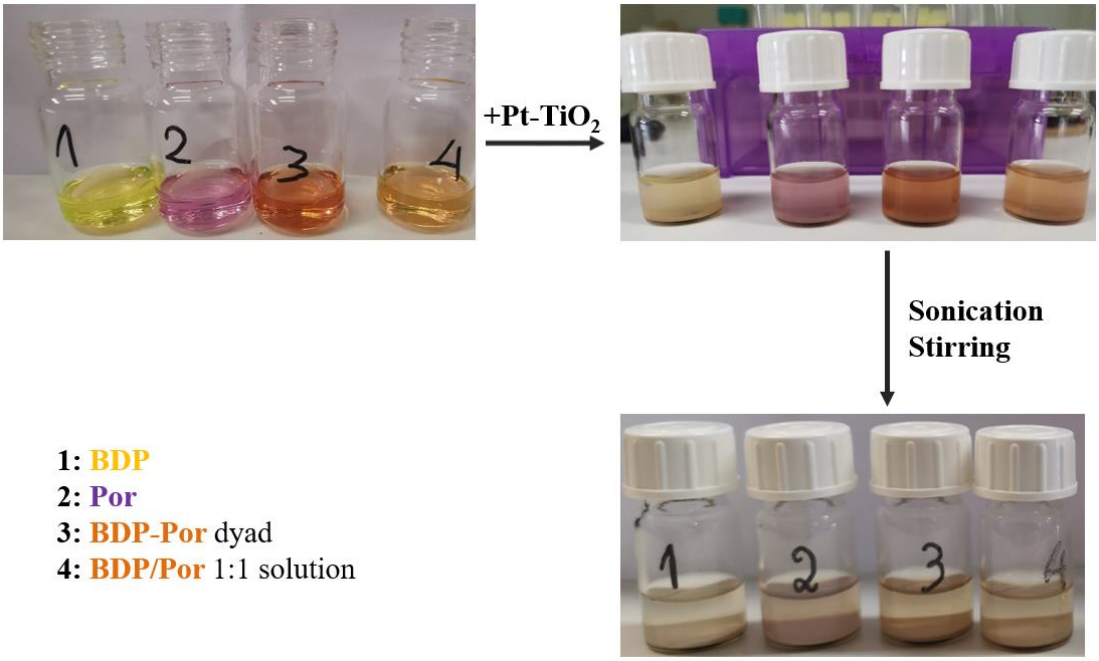

Figure S7. Adsorption methodology before the photocatalysis experiments of:

1. **BDP**, 2. **Por**, 3. **BDP-Por** dyad and 4. **BDP/Por** 1:1 mixture.

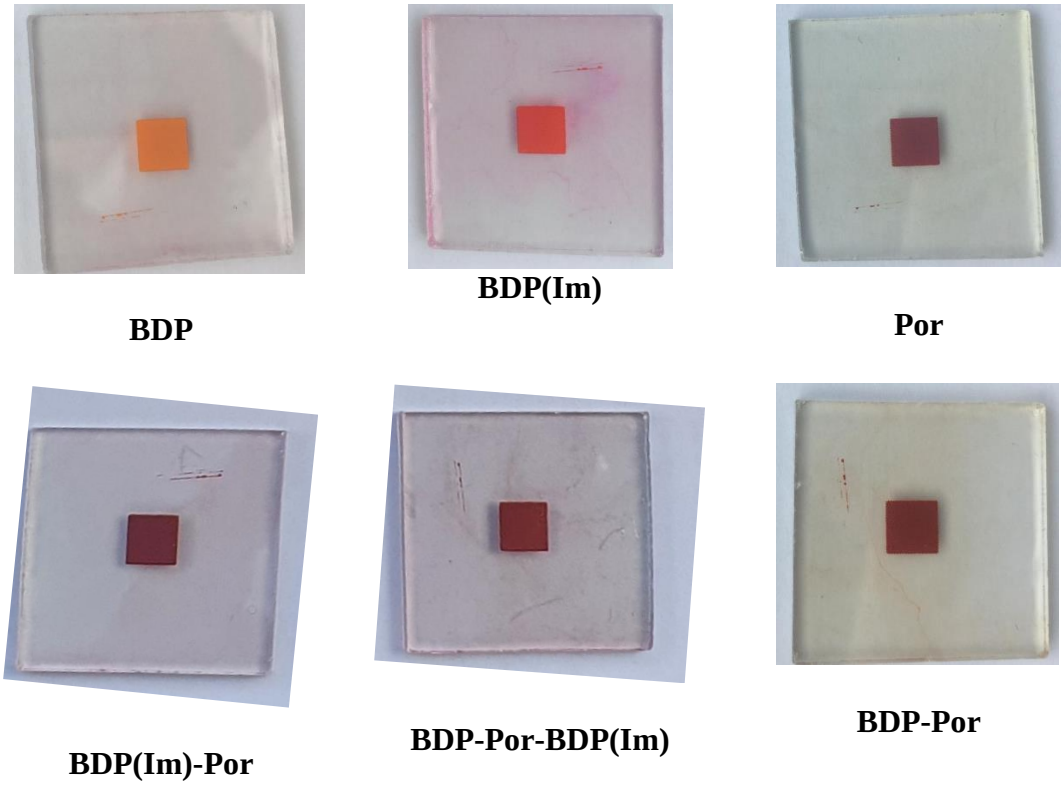

Figure S8. Pictures of the TiO_2 electrodes used for chopped light experiments.

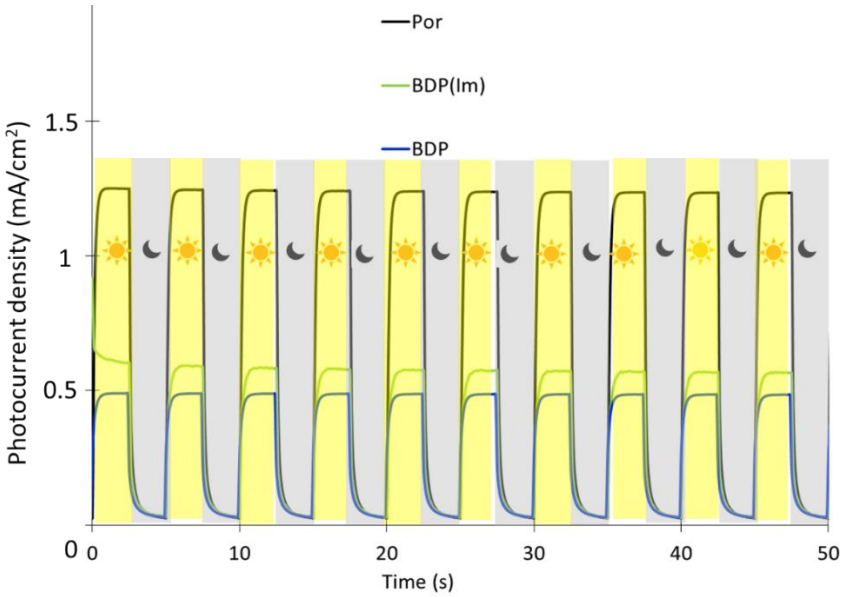

Figure S9. Chopped light voltammetry measurements recorded under white light irradiation (350 W/m^2) of the sensitizers chemisorbed on TiO_2 film with the aqueous electrolyte containing [AA] = 1 M, [$LiClO_4$] = 0.1 M at pH = 4. Applied potential = 0 V *vs.* SCE.

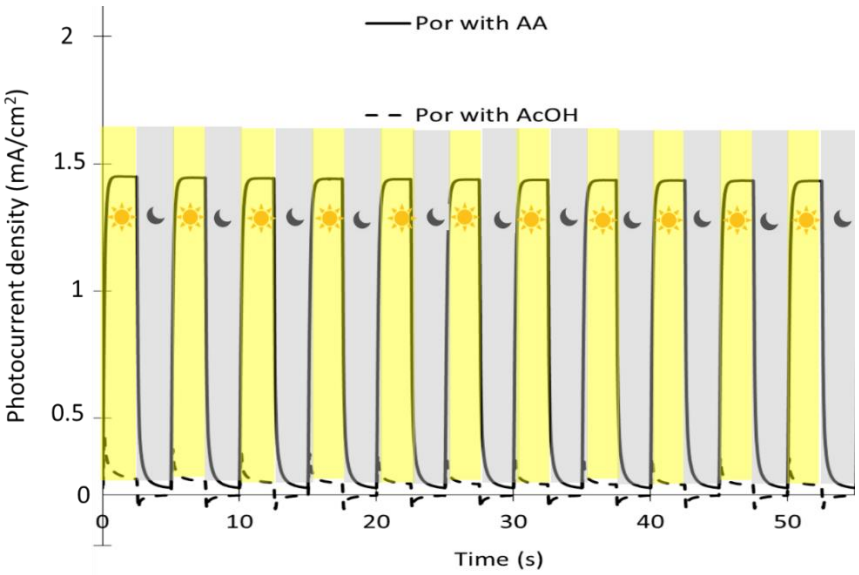

Figure S10. Chopped light voltammetry measurements recorded under white light irradiation (350 W/m^2) of Por chemisorbed on TiO_2 film with the aqueous electrolyte containing [AA] = 1 M, [$LiClO_4$] = 0.1 M at pH = 4 (straight line) or with the aqueous electrolyte containing [AcOH] = 0.1 M, [$LiClO_4$] = 0.1 M at pH = 4 (dashed line). Applied potential = 0 V *vs.* SCE.

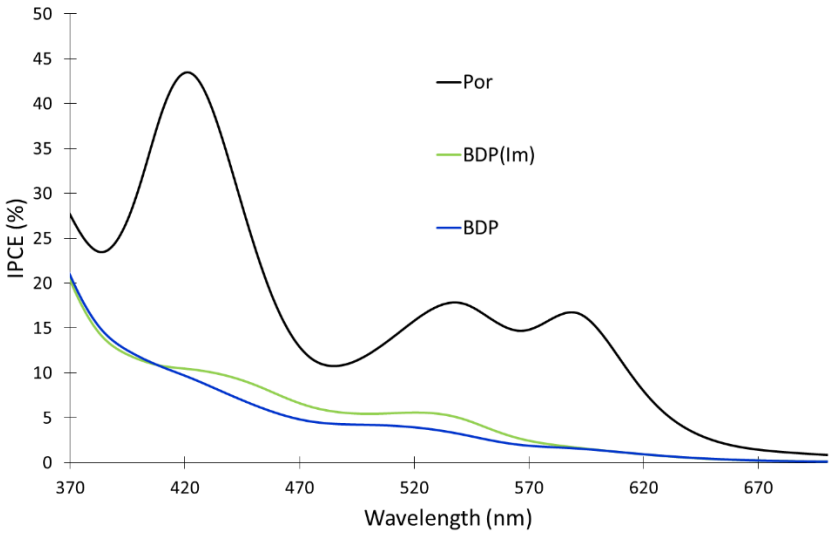

Figure S11. IPCE spectra recorded at applied potential 0 V *vs.* SCE of the sensitizers chemisorbed on TiO_2 film with the aqueous electrolyte containing [AA] = 1 M, [$LiClO_4$] = 0.1 M at pH = 4.

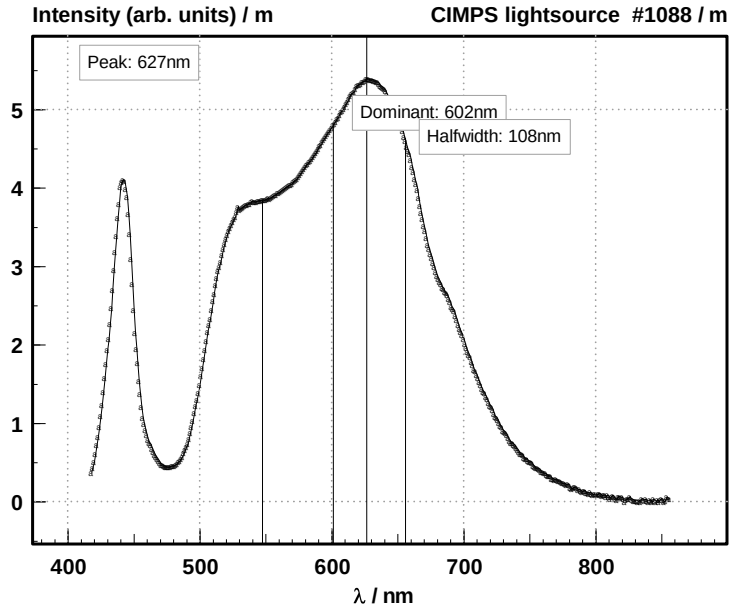

Figure S12. Spectrum of the white light lamp used for spectroelectrochemical measurements.

Transient Absorption Studies.

Transient absorption measurements based on nanosecond laser photolysis were performed on the TiO_2 and Pt-TiO_2 particles. The results of the photoexcitation of TiO_2 nanoparticles are commonly discussed in form of the formation of an electron-hole pair with an electron residing in the conduction band (e_{CB}^-) and a hole residing in the valence band (h_{VB}^+). This electron-hole pair is rapidly decaying on the femtosecond time scale, either recombining or the charges become captured and subsequently localized in trap states resulting from structural non-periodicity induced disorders in the TiO_2 lattice, for example, undercoordinated ions (Ti^{4+}) and oxygen vacancies.[3,4] Such trap states can act as both centers for electron-hole recombination or, in contrary, might help enhancing the charge separation and thus supporting the proceeding of slow interfacial redox reactions.[5,6] Depending on the energetic position of the defect-related energy states relative to the band gap, they are referred to as

shallow or deep-level taps. Shallow traps are positioned close to the edge of the respective band (conduction band for e^-, within 0-0.05 eV below the band edge;[7] valence band for h^+), whereas deep-level trap states are located towards the middle of the energy gap and are considered to be predominantly responsible for (non-radiative) recombination events.[3] Commonly discussed trapping routes and states within the TiO_2 lattice or terminal at the surface, as well as interaction with at the surface adsorbed electron donor (D) and electron acceptor (A) molecules are depicted in Scheme S2.:

Scheme S2: Overview over the most important processes in TiO_2 upon photoexcitation and a rough timeframe in which these processes occur.[3]

$$TiO_2 + hv \rightarrow TiO_2(e_{CB}^- + h_{VB}^+) \quad \sim 100 \text{ fs}$$

$$Ti^{4+} + e_{cb}^- \rightarrow Ti^{3+} \quad \sim 100 \text{ fs}$$

$$Ti\text{-}OH + h_{VB}^+ \rightarrow Ti\text{-}OH^{\bullet+} \quad \sim 100 – 200 \text{ fs}$$

$$Ti\text{-}OH + h_{VB}^+ \rightarrow Ti\text{-}OH^{\bullet+} \quad \sim 100 – 200 \text{ fs}$$

$$Ti\text{-}O\text{-}Ti + h_{VB}^+ \rightarrow Ti\text{-}O^{\bullet+}\text{-}Ti \quad \sim 100 – 200 \text{ fs}$$

$$Ti\text{-}OH + h_{VB}^+ \rightarrow Ti\text{-}OH^{\bullet+} \quad \sim 100 – 200 \text{ fs}$$

$$Ti\text{-}OH^{\bullet+} + e_{CB}^- \rightarrow Ti\text{-}OH + hv \text{ or heat } \sim 100 \text{ ps} – 10 \text{ ns}$$

$$Ti\text{-}O^{\bullet+}\text{-}Ti + e_{CB}^- \rightarrow Ti\text{-}O\text{-}Ti + hv \text{ or heat } \sim 100 \text{ ps} – 10 \text{ ns}$$

$$Ti^{3+} + Ti\text{-}OH^{\bullet+} \rightarrow Ti^{4+} + Ti\text{-}OH \quad >> 10 \text{ ns}$$

$$Ti^{3+} + Ti\text{-}O^{\bullet+}\text{-}Ti \rightarrow Ti^{4+} + Ti\text{-}O\text{-}Ti \quad >> 10 \text{ ns}$$

$$e_{cb}^- + A \rightarrow A^{\bullet-} \quad > 10 \text{ ns}$$

$$Ti^{3+} + A \rightarrow Ti^{4+} + A^{\bullet-} \quad >> 10 \text{ ns}$$

$$Ti\text{-}OH^{\bullet+} + D \rightarrow Ti\text{-}OH + D^{\bullet+} \quad 100 \text{ ps} - 10 \text{ ns}$$

$$Ti\text{-}O^{\bullet+}\text{-}Ti + D \rightarrow Ti\text{-}O^{\bullet+}\text{-}Ti + D^{\bullet+} \qquad 100\ ps\text{-}10\ ns$$

Turning to the nanosecond laser photolysis transient absorption measurements of the TiO_2 nanoparticles in acetonitrile (Figure S13) a broad transient absorption band with a maximum around 450 nm covering the UV and visible spectrum is discernible.

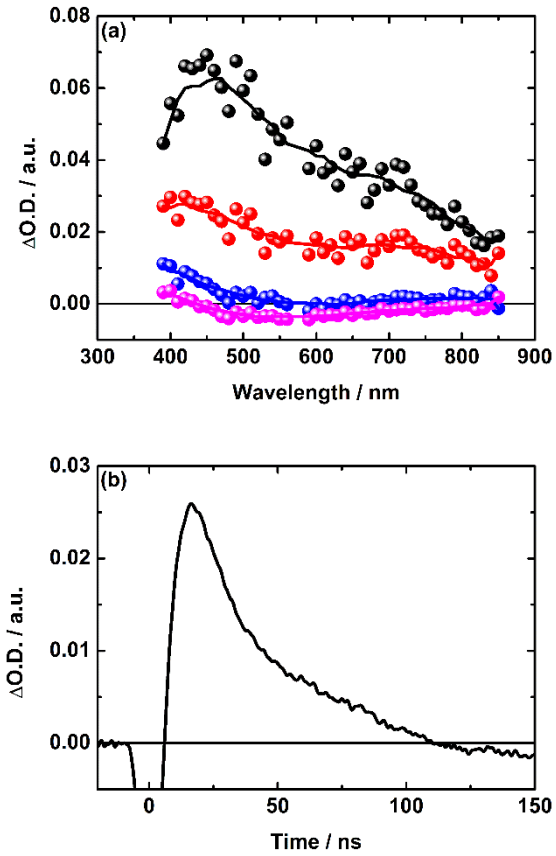

Figure S13. (a) Nanosecond transient absorption spectra of the TiO_2 nanoparticles in nitrogen saturated acetonitrile, photoexcited at 266 nm (4 mJ / pulse, 5 ns FWHM) 25 ns (black) 50 ns (red), 100 ns (blue) and 125 ns (magenta) after the laser pulse. **(b)** Corresponding time absorption profile at 450 nm. Please note, no date below 390 nm were recordable due to the saturation of the detector due to emission originating from the excitation recombination.

This transient absorption band is according the Scheme S2 best described as a superimposition of the transient absorption of conduction band electrons trapped in

Ti^{3+} centers which absorptions cover the whole optical spectrum and trapped holes dominating the spectrum in the blue region.[8] These transient absorptions decay with a lifetime of 30 ns. Taking a very in depth look at the spectra at 125 ns after the laser pulse a negative signal is discernable between 400 and 800 nm. Since there is no ground state absorption, the most feasible rational are radiative electron-hole recombination, self-trapped excitons localized on TiO_6 octahedra, or the emissive reaction of free or shallowly trapped charges with their (deeply) trapped counterpart.[3,9] When changing from acetonitrile to water as "solvent", the transient absorption spectrum is still dominated by an absorption that covers the whole UV and visible spectrum (Figure S14) originating form trapped holes and trapped electrons – which is in line with the literature.[3,8] These transient absorptions decay with a lifetime of 60 ns leaving a very small residual transient absorption which may relate to charge charrier in deeper level trap states. When ethanol is added – which is a well-established hole quencher[10] – a shortening of this lifetime is observed (compare Figure S14b black and red line).

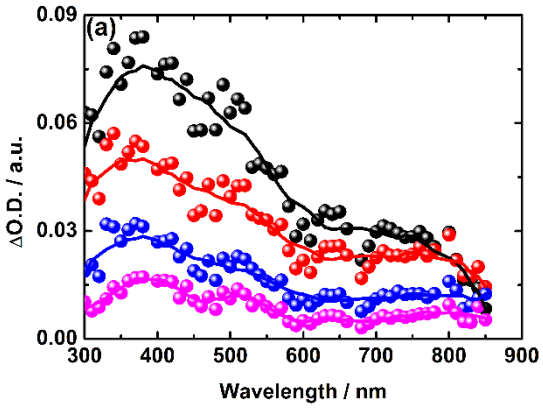

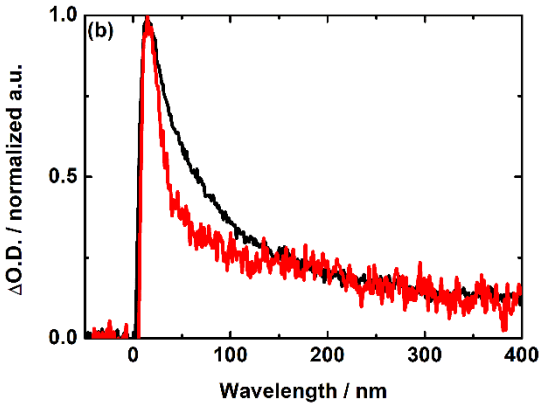

Figure 14. (a) Nanosecond transient absorption spectra of the TiO_2 nanoparticles in nitrogen saturated water, photoexcited at 266 nm (4 mJ / pulse, 5 ns FWHM) 25 ns (black), 50 ns (red), 100 ns (blue) and 200 ns (magenta) after the laser pulse. **(b)** Corresponding time absorption profile at 370 nm (black). The red time profile was measured under the same conditions but with the addition of 5 vol% ethanol.

Turning to the platinum particle coated TiO_2 (Pt-TiO_2) the photoexcitation of aqueous dispersions with 266 nm nanosecond laser pulses resulted in a transient absorption spectrum dominated by a maximum around 370 nm indicating towards trapped holes,[8] while transient absorptions relating to (trapped) electrons are absent. The missing of transient absorption relating to negative charges is not surprising since it is known in the literature that the electron moves into the conduction band of the metal and thus act as co-catalyst in proton reduction reactions.[11-14] Taken a more detailed look at the time profile at 370 nm (Figure S15) one observes a decay within the first 1 µs followed by a long-lived transient absorption without substantial spectral changes. This first decay process is best explained with a shift of trapped hole into deeper trap states which show a lifetime in the microsecond time range, but due to the low intensity (~1 mV on a 180 mV baseline) we were unable to make a precise determination due to baseline instabilities in the same order of magnitude at detection times in the 100 µs range, so that we prefer not to state any value here.

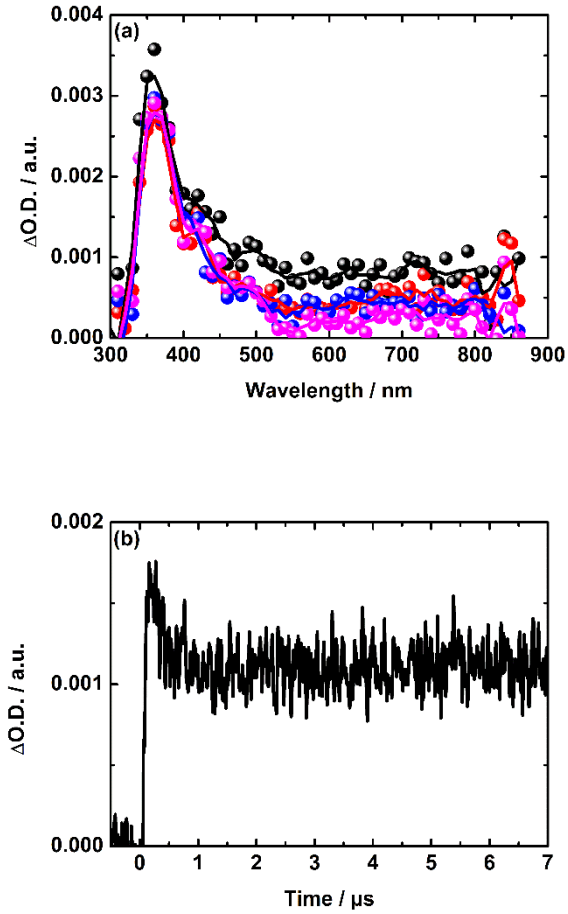

Figure S15. (a) Nanosecond transient absorption spectra of the Pt-TiO_2 nanoparticles in nitrogen saturated water, photoexcited at 266 nm (4 mJ / pulse, 5 ns FWHM) 500 ns (black), 1 μs (red), 2 μs (blue) and 5 μs (magenta) after the laser pulse. **(b)** Corresponding time absorption profile at 370 nm.

Concerning the complete system, that is the dyad attached to the Pt-TiO_2 particle (**BDP(Im)-Por@Pt-TiO_2**) the compound disintegrated during the measurements due to the intense photon flux by our laser system and due to the holes formed at the Pt-TiO_2 degrading the dyad.

References

1. P.-Y. Ho, Y. Wang, S.-C. Yiu, W.-H. Yu, C.-L. Ho, S. Huang, Starburst Triarylamine Donor-Based Metal-Free Photosensitizers for Photocatalytic Hydrogen Production from Water, Org. Lett. **2017**, 19, 1048.
2. J. S. Lindsey, S. Prathapan, T. E. Johnson, R. W. Wagner, Porphyrin building blocks for modular construction of bioorganic model systems, Tetrahedron 1994, 30, 8941.
3. J. Schneider, M. Matsuoka, M. Takeuchi, J. Zhang, Y. Horiuchi, M. Anpo, D. W. Bahnemann, Understanding TiO2 photocatalysis: mechanisms and materials, Chem. Rev. **2014**, 114, 9919.
4. J. Schneider, D. W. Bahnemann, Undesired Role of Sacrificial Reagents in Photocatalysis, J. Phys. Chem. Lett. **2013**, 4, 3479.
5. A. Litke, E. J. M. Hensen and J. P. Hofmann, Role of Dissociatively Adsorbed Water on the Formation of Shallow Trapped Electrons in TiO 2 Photocatalysts, J. Phys. Chem C, **2017**, 10153–10162.
6. F. Amano, M. Nakata, A. Yamamoto and T. Tanaka, Effect of Ti3+ Ions and Conduction Band Electrons on Photocatalytic and Photoelectrochemical Activity of Rutile Titania for Water Oxidation, J Phys. Chem C, **2016**, 6467.
7. S. Kohtani, A. Kawashima and H. Miyabe, Reactivity of Trapped and Accumulated Electrons in Titanium Dioxide Photocatalysis, Catalysts, **2017**, 303.
8. P. Zawadzki, Absorption spectra of trapped holes in anatase TiO2, J. Phys. Chem C, **2013**, *117*, 8647.
9. H. Tang, H. Berger, P. E. Schmid, F. Lévy and G. Burri, Photoluminescence in TiO2 anatase single crystals, Solid State Commun., **1993**, 847.
10. Y. D. Iorio, M. E. Aguirre, M. A. Brusa and Maria A. Grela, Surface chemistry determines electron storage capabilities in alcoholic sols of titanium dioxide nanoparticles. A combined FTIR and room temperature EPR investigation, J. Phys. Chem. C, 2012, 116, 9646.
11. Y. Ham, T. Hisatomi, Y. Goto, Y. Moriya, Y. Sakata, A. Yamakata, J.Kubota, K. Domen, Flux-mediated doping of SrTiO3 photocatalysts for efficient overall water splitting, J. Mater. Chem. A **2016**, 4, 3027.

12. Y. Goto, T. Hisatomi, Q. Wang, T. Higashi, K. Ishikiriyama, T. Maeda, Y. Sakata, S. Okunaka, H. Tokudome, M. Katayama, S. Akiyama, H. Nishiyama, Y. Inoue, T. Takewaki, T. Setoyama, T. Minegishi, T. Takata, T. Yamada, K. Domen, A Particulate Photocatalyst Water-Splitting Panel for Large-Scale Solar Hydrogen Generation, Joule **2018**, 2, 509.
13. S. Chen, T. Takata, K. Domen, Particulate photocatalysts for overall water splitting, Nat. Rev. Mater. **2017**, 2, 17050.
14. N. Liu, S. Mohajernia, N. T. Nguyen, S. Hejazi, F. Plass, A. Kahnt, T. Yokosawa, A. Osvet, E. Spiecker, D. M. Guldi, P. Schmuki, Long-Living Holes in Grey Anatase TiO2 Enable Noble-Metal-Free and Sacrificial-Agent-Free Water Splitting, ChemSusChem, **2020**, 13, 4937-4944.